Mechanical Properties of Model Polyethylenes: Tensile Elastic Modulus and Yield Stress

Buckley Crist,* Christopher J. Fisher, and Paul R. Howard

Departments of Chemical Engineering and Materials Science and Engineering, Northwestern University, Evanston, Illinois 60208. *Received July 15, 1988; Revised Manuscript Received October 6, 1988*

ABSTRACT: Room temperature tensile modulus E and yield stress σ_y are presented for linear polyethylene and model ethylene–butene-1 copolymers both with and without long-chain branching. Analyses of these data focus on apparent crystallinity dependence and absolute values of E and σ_y. Most of the variation in E is due to a strong increase in the amorphous modulus with crystal thickness l_c caused by suppression of the mechanical α_1 relaxation process. Yield stress is modeled in terms of nucleation of [001] screw dislocations leading to $(hk0)[001]$ slip in lamellar crystals. Experimental strengths are accounted for quantitatively in the range 175 K $\leq T \leq$ 260 K. Deviations at higher and lower temperatures are ascribed to chain dynamics in semicrystalline polyethylene.

Introduction

The mechanical behavior of ductile polymers, either glassy or semicrystalline, can be divided into various categories: elastic or linear viscoelastic response at small strains, yielding or the onset of irreversible deformation, the post-yield or flow region, and failure. Polyethylene, in the form of a linear homopolymer, random copolymers containing noncrystallizable repeats, or molecules with long-chain branching, presents an interesting range of properties. These are achieved for the most part by varying the degree of crystallinity by thermal history, comonomer content and distribution, and molecular weight and molecular weight distribution. Macroscopic orientation also has a strong effect on mechanical properties.

This work is concerned with the tensile properties of isotropic polyethylenes at room temperature. Model polymers are employed, these having well-defined molecular weights (and for the most part, quite narrow molecular weight distributions), uniform ethyl branch concentrations, and long-chain branching (three- and four-arm star molecules). What can be termed small strain properties, i.e., tensile modulus and yield stress, are discussed in this paper. Large scale plastic deformation and failure are the subjects of a companion work.[1]

It has long been recognized that room temperature elastic moduli[2-8] and yield stress[2-5,9-12] increase with the crystallinity of polyethylene. The response of the elastic modulus to crystallinity appears to be understood, at least in a qualitative sense, in terms of the two-phase model for a semicrystalline polymer. Regardless of the longstanding controversy regarding the glass transition in polyethylene,[7,13] it is generally agreed that the noncrystalline portion of polyethylene is liquidlike or "rubbery" at room temperature. While the elastic constants of this phase may depend on morphology, temperature, and the like, there is no doubt that noncrystalline polyethylene at room temperature is substantially more compliant than the crystallites. Furthermore, reasonable estimates exist for elastic properties in the limits of complete and no crystallinity. In this paper we will refer to the volume fraction crystallinity α, which is most conveniently derived from sample density.

The best experimental determination of the crystalline modulus for isotropic polyethylene is that of Illers,[6] who measured shear modulus G as a function of temperature and crystallinity (α = 0.45–0.96). Modest extrapolation to α = 1 yields G_c = 3.7 GPa at −160 °C and G_c = 2.7 GPa at 20 °C. Theoretical estimates of elastic moduli have been obtained via potential functions parameterized to duplicate the equilibrium crystal structure of polyethylene.[14-16] Results calculated by assuming a uniform stress (Reuss average) throughout the isotropic polycrystalline aggregate are shown in Table I and are seen to agree to better than 20% with Illers' experimental values. (Constant strain or Voigt average G_c is about eight times larger, clearly incompatible with experiment.) Note also that the relative magnitude of the temperature dependence of G_c is reproduced nicely by the calculations of Odajima and Maeda.[14] The bulk modulus K (inverse of the isothermal compressibility) has been measured at and above room temperature by Hellwege et al.[17] for polyethylenes of varying crystallinity. This quantity is less sensitive to α than are shear or tensile moduli, permitting reliable extrapolations to obtain both K_c and K_a. Experimental and calculated (Reuss average) values of K_c are again in accord, confirming our certainty that the elastic behavior of fully crystalline polyethylene is understood.

Table I
Elastic Constants of Isotropic Polyethylene (GPa)

			calcd		
		exptl	ref 14	ref 15	ref 16
		Crystalline PE			
G_c	−160 °C	3.7[a]	3.03	3.66	4.09
	20 °C	2.7[a]	2.23		
K_c	−160 °C		6.87	10.1	9.87
	20 °C	5.8[b]	5.03		
E_c	−160 °C		7.92	9.81	10.8
		Amorphous PE			
G_a	−160 °C		2[d]		
	20 °C	$(2 \pm 1) \times 10^{-3}$[c]	0.1[d]		
K_a	20 °C	1.8[b]			

[a] Reference 6. [b] Reference 17. [c] Reference 7. [d] Reference 19.

The situation with the amorphous component is less clear. Krigas et al.[7] extrapolated the rubbery plateau modulus of molten polyethylene to room temperature and also extrapolated room temperature tensile modulus E to α = 0 with a series of low-crystallinity model copolymers of ethylene. Both methods yield $G_a \approx 2$ MPa, a figure which is 3 orders of magnitude smaller than G_c. While no ab initio theory exists for the modulus of uncross-linked melts, the correspondence between tensile behavior at low α and melt elasticity is consistent with rubberlike elasticity manifested through entanglements.[18] Included in Table I are values of G_a calculated by Boyd[19] by fitting Illers' results to a model which uses constant stress (Reuss) averaging for an assembly of anisotropic lamellar polyethylene crystals separated by isotropic amorphous regions. The value of G_a at room temperature, which actually represents a model-dependent extrapolation to α = 0 from the range α = 1.0–0.5, is 2 orders of magnitude larger than result of Krigas et al.

0024-9297/89/2222-1709$01.50/0

This discrepancy between properties of amorphous polyethylene leads to the issue of how the elastic properties depend on crystallinity and other aspects of the morphology of semicrystalline polymers. One of the earliest treatments is that of Krigbaum et al.[20,21] who considered the elastic modulus of polyethylene to result from deformation of amorphous "tie molecules" obeying inverse Langevin statistics. Their model is effectively a Reuss average in which the compliance of the crystals is zero, and the compliance of the noncrystalline regions drops as α is increased or as temperature is decreased in the range between T_m and T_g. A simpler approach is to invoke some sort of two-phase model in which the properties of each component are independent of crystallinity α. The first such analysis for isotropic semicrystalline polymers was an empirical logarithmic mixing law proposed by Gray and McCrum:[22]

$$\log G = \alpha \log G_c + (1 - \alpha) \log G_a \quad (1)$$

This expression was shown to lie between general constant stress and constant strain bounds for arbitrary two-phase systems composed of *isotropic* phases. Since polyethylene crystals are extremely anisotropic, it is not surprising that eq 1 fails to account for the data of Illers,[6] particular above room temperature. Other mixing laws have been considered by Boyd,[23] culminating in the lamellar model[19] which is based on sound mechanical principles and describes quite well Illers' results with α-independent values of G_c and G_a. Phillips and Patel[24] and Popli and Mandelkern[9] have employed a very simple linear relation which can be written as

$$G = \tfrac{3}{8}[\alpha G_c + (1 - \alpha)G_a] \quad (2)$$

This expression appears to work, perhaps fortuitously, with linear polyethylenes over the range $\alpha \approx 0.60$–0.85. Considering the many simplifications inherent in eq 2, its inadequacy for polyethylene of lower crystallinity is not unexpected.

Yielding in semicrystalline polymers such as polyethylene is imperfectly understood, particularly the positive dependence of yield stress σ_y on crystallinity. Again in the spirit of two-phase composite response, Matsuoka[25] treats initial deformation and yielding in terms of nonlinear viscoelasticity, with implicit emphasis on the noncrystalline component. But yielding, i.e., the onset of plastic deformation, requires irreversible shear of the crystallites. This has been demonstrated conclusively by Young et al.[26] by X-ray studies of specially oriented linear polyethylene deformed in plane strain compression. There it was found that interlamellar shear resulting from deformation of the amorphous regions between crystals was recovered after unloading. Chain slip within the crystals along the [001] direction (intracrystalline shear) was irreversible, commencing with macroscopic yielding and continuing at a critical resolved shear stress of 6–15.5 MPa, which varies with density (crystallinity). It is logical to assume that the same situation obtains for uniaxial tensile deformation of isotropic polyethylene. Indeed, observed tensile yield stress is in the range of 22–32 MPa over the density range of 0.95–0.97 g/cm^3 (cf. the compendium in ref 9), which is consistent with resolved shear reported by Young et al.

The absolute magnitude of the yield stress has received some attention. It is well established that the ratio τ_{max}/G, where τ_{max} corresponds to the shear stress for the onset of plastic deformation by slip, is about 0.16 for perfect crystals and 0.10 for amorphous (glassy) substances.[27] Young[28] and Shadrake and Guiu[29] have treated the observation that $\tau_{max}/G \approx 5 \times 10^{-3}$ in polyethylene at room temperature in terms of thermally activated screw dislocations being generated in thin lamellar crystals. These would provide the mechanism for $(hk0)[001]$ slip. This dislocation model predicts that shear strength is reduced by decreasing crystal thickness or increasing temperature. The details of these model calculations disagree in some aspects, as will be discussed below. Nevertheless, such dislocations are instructive when considering changes in yield stress caused by varying crystallinity (crystal thickness) and temperature.

An alternative explanation for the dependence of σ_y on temperature and crystallinity has been presented by Popli and Mandelkern.[9] Those authors rely on an apparent linear relation between σ_y and l_c, the most probable crystal thickness, to support the notion that macroscopic yielding is caused by local melting and recrystallization in semicrystalline polyethylene. This idea has also been used to account for certain aspects of morphology changes, particularly the "long period" characteristic of semicrystalline polymers, after plastic deformation.[30] Even qualitative estimates of the magnitude of σ_y, its dependence on l_c, etc. are not presented for this model.

We report here room temperature tensile modulus E and yield stress σ_y measurements on isotropic polyethylene (linear polyethylene and model copolymers) having well-characterized chemical microstructures and morphologies. Particular attention is paid to the dependence of E and σ_y on crystallinity. It is shown that crystal thickness l_c has an important role in determining the mechanical behavior of polyethylene at small strains.

Experimental Section

Materials. Polymers are of three types: linear polyethylene fractions and whole polymer (National Bureau of Standards Reference Materials), linear hydrogenated polybutadiene, and star-shaped hydrogenated polybutadiene. Hydrogenated polybutadiene (HPB) is prepared by quantitative saturation of anionically polymerized butadiene. HPB samples were synthesized locally or generously supplied by the Phillips Petroleum Co.; these polymers contain about 20 ethyl branches per 1000 backbone C atoms (resulting from 1–2 additions of butadiene) and are model copolymers of ethylene and butene-1.[7] Molecular weight distributions are very narrow, with $M_w/M_n = 1.05$–1.10. The star polymers may contain up to ca. 10% uncoupled arms. Synthesis and characterization of HPB have been described previously.[31-33]

Bimodal blends of different molecular weight HPB of the same type were prepared by dissolving in refluxing cyclohexane and precipitating in methanol. These blends were stabilized by the addition of Irganox 1010, then thoroughly washed, and dried.

Linear polyethylene fractions are called PE32 and PE120, where the suffix is the molecular weight in thousands. The whole polymer is designated PE52W. Linear HPB is described by L and the molecular weight, while the three-arm and four-arm stars are indicated by 3S and 4S, respectively. Bimodal blends of the linear and star HPB's are identified by component molecular weights and the weight fraction of the low molecular weight species; e.g., L186/13.91 is a mixture of the $M = 186\,000$ linear HPB with 91 wt % of the $M = 13\,300$ polymer.

Samples for tensile testing were compression molded at suitable temperatures ranging from 110 to 190 °C and quenched in ice water. The linear HPB films were given an alternative thermal history, slow-cooling from the melt at a rate of less than −0.2 °C/min through the crystallization range near 90 °C. PE120 was also slowly cooled at different rates to increase the crystallinity range.

All polyethylenes and HPB's are semicrystalline with conventional lamellar microstructure and, except as noted, spherulitic. Densities, measured in a gradient column, are reported in Tables II and III. For the two polyethylene fractions there is the expected decrease in crystallinity with increasing molecular weight (from $\alpha = 0.63$ to $\alpha = 0.51$ based on crystalline density $\rho_c = 1.003$ g/cm^3 and amorphous density $\rho_a = 0.850$ g/cm^3 at 25 °C[17,34]). Melting temperature evaluated by DSC (5 °C/min after cooling at 10

Table II
Physical and Engineering Tensile Properties of Polyethylenes and Hydrogenated Polybutadienes

polymer[a]	M_w, g/mol	M_w/M_n	ρ, g/cm^3	E, MPa	σ_y, MPa
PE32	32 100	1.11	0.944	800	17.3
PE120	119 600	1.19	0.928	410	14.0
			0.934	500	13.8
			0.944	830	19.5
			0.949	1000	22.0
			0.953	1100	24.3
PE52W	52 000	2.89	0.946	650	15.4
L13	13 300	<1.05	0.928	300	
			0.929	310	
L44	43 600	<1.05	0.912	100	5.8
			0.922	260	9.1
L61	60 700	<1.05	0.906	62	4.5
			0.914	150	6.7
L96	95 600	<1.05	0.906	77	4.5
L124	124 000	<1.05	0.903	54	3.8
L150	150 000	<1.05	0.903	76	4.5
			0.911	140	6.0
L186	186 000	<1.05	0.905	55	3.8
			0.911	100	5.2
L199	199 000	<1.05	0.902	68	3.9
			0.908	110	5.8
3S23	22 700	1.1	0.910	73	4.1
3S40	40 400	1.1	0.910	72	3.8
3S66	66 400	1.1	0.909	72	3.9
3S104	103 700	1.1	0.909	67	3.7
3S161	161 000	1.1	0.906	62	3.7
4S160	159 700	1.1	0.907	72	4.5

[a] First entry for each polymer is quenched crystallized. Subsequent entries are for slowly cooled samples.

Table III
Physical and Engineering Tensile Properties of Bimodal Blends

polymer[a]	M_w, g/mol	M_w/M_n	ρ, g/cm^3	E, MPa	σ_y, MPa
L186/13.91	28 800	1.99	0.928	300	
			0.930	330	
L186/13.80	47 800	2.94	0.924	210	7.7
			0.929	360	
L186/13.70	65 100	3.54	0.919	170	7.6
			0.927	300	10.5
L186/13.60	82 400	3.89	0.918	120	6.1
			0.929	280	9.2
L186/13.30	134 000	3.54	0.910	82	5.0
			0.923	210	8.3
3S161/23.80	50 400	1.84	0.910	68	3.9
3S161/23.60	78 000	2.26	0.909	66	4.1
3S161/23.40	105 700	2.26	0.908	65	4.1
3S161/23.20	133 000	1.84	0.908	61	4.0

[a] First entry for each blend is quench crystallized. Second entry is for slowly cooled sample.

°C/min) was 133 ± 0.5 °C for all these linear polyethylenes. Spherulite radii from H_v light scattering were in the range 2–5 μm with no discernible trend with molecular weight. The small-angle X-ray long period was about 200 Å for PE32 and PE52W. The long period of PE120 ranged from 250 Å (quenched) to 390 Å (slowly cooled).[35]

Linear HPB has a similar decrease of density with increasing molecular weight, with crystallinity dropping from $\alpha = 0.58$ (L13) to $\alpha = 0.37$ (L199), based on a measured crystalline density $\rho_c = 0.986$ g/cm^3[35] and $\rho_a = 0.850$ g/cm^3. The melting temperature decreases from 108 °C (L13) to 102 °C (L150) with increasing molecular weight, paralleling the density or crystallinity. Slow cooling causes a very modest increase in density; this insensitivity is typical of copolymers in which crystallinity is determined by branch concentration.[36] The long period is typically 140 Å, increasing to 150 Å after slow cooling.[35,37] Depolarized light scattering indicates spherulites with radii 1–3 μm in all slow cooled linear HPB's and quenched samples with $M \leq 95\,600$.

Bimodal blends may be problematic because of segregation of different molecular weight chains, particularly during slow cooling.

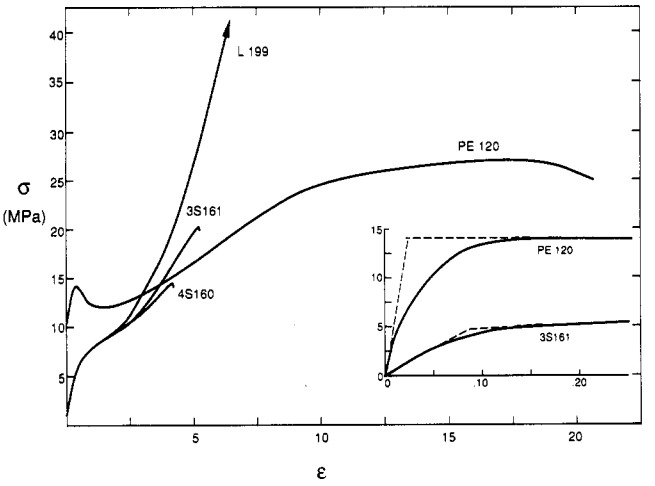

Figure 1. Tensile stress–strain curves for representative polyethylenes and HPB's. Stress and strain are based on undeformed sample dimensions. Insert shows method for evaluating yield stress σ_y.

Small-angle neutron scattering can provide some information on this issue. Tanzer et al.[38] have shown that ideal molecular mixing is achieved with quenched blends of linear HPB's differing in molecular weight by a factor of 5, though there is some indication that slow cooling may lead to partial segregation. It is noted here that density in both quenched and slow-cooled blends of linear HPB is enhanced, being fairly close to that of the low molecular weight component L13, particularly in the slow-cooled blend series L186/13 (Table III).

The 3S HPB samples have densities (crystallinity of 0.43) which are remarkably insensitive to molecular weight over the range studied. The peak melting temperature is 102 °C, and the melting endotherm is broad, both features being the same as those in linear HPB having the same branch content. Spherulite radii of 5–8 μm were observed for $M \leq 66\,400$. Higher molecular weight S3 and S4 and all S3 blends had no characteristic "cloverleaf" H_v pattern.

Tensile Testing. Microtensile specimens were cut from the films (gage length 19.5 mm, width 2.0 mm, thickness about 0.13 mm). Testing was done with a table model Instron at room temperature (23 ± 2 °C). Particular care was paid to alignment of grips and specimen to achieve uniaxial elongation. Elastic modulus was measured from initial force–elongation response at a strain rate of 2.2×10^{-3}/s. The maximum stress used in this procedure was about 1.5 MPa, corresponding to strains ranging from ~0.2% (PE) to 2.5% (L, 3S, 4S). No nonlinearity in force–displacement[3] was observed over this range, though the small samples used here are not suitable for detailed examination of such effects.

After the modulus measurement, the sample was unloaded and subsequently deformed at a nominal strain rate of 4.4×10^{-3}/s (11×10^{-3}/s for the linear HPB fractions and blends). Three to five replicate specimens were run for each sample. Representative engineering stress–strain curves are shown in Figure 1. The insert shows the method of tangents used to define the yield stress σ_y. This permits a consistent analysis to be applied to samples which displayed a load drop (sharp neck) and those that did not. The yield stress determined in this manner is typically 10% less than the peak stress in polyethylene and HPB which necked conspicuously.

Results and Discussion

Tensile Modulus. Modulus measurements involve tensile strains on the order of 0.01, so no direct correlation between E and polymer molecular weight is expected. It is clear from the compilations in Table II and III and the graphical summary in Figure 2 that density appears to be the dominant parameter controlling the elastic modulus. Short-chain branching and, to a lesser extent, increased molecular weight lead to lower density and modulus, in accord with previous studies of polyethylene and co-

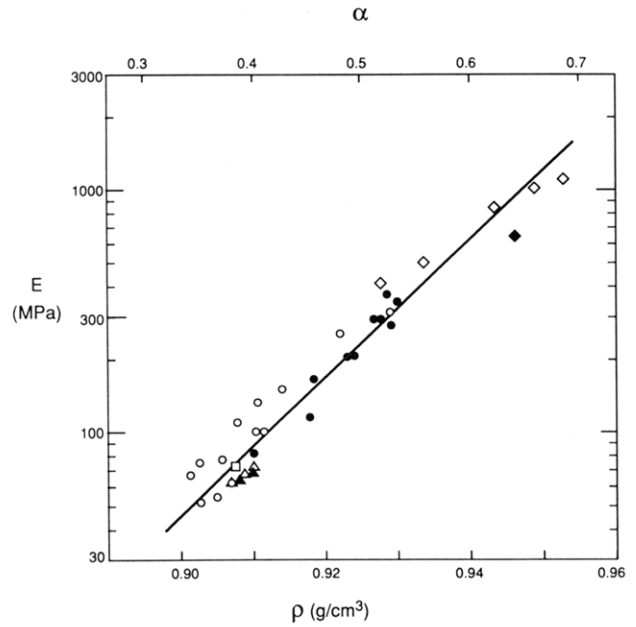

Figure 2. Dependence of tensile modulus E on sample density and crystallinity. Line is linear least-squares fit to data. Symbols are for PE (◇), linear HPB (○), 3S HPB (△), and 4S HPB (□). Solid symbols are for polydisperse samples.

polymers. The ability to vary density by changing molecular weight or molecular weight distribution is strongly suppressed by long-chain branching. In the S3 samples chain mobility is effectively slowed (with respect to the cooling schedule used in these experiments) for even the lowest molecular weight 3S13.

Figure 2 shows a scatter of about ±15% in elastic modulus at any particular density. This is beyond the confidence limits of the measurements (±5% for E, ±0.5% for ρ) and presumably is real, though no universal trend is apparent with respect to either thermal history or molecular weight. Data for all the polyethylenes are adequately described by the relation corresponding to the solid line in Figure 2. The correlation coefficient for the fit is 0.974, reflecting for the most part the scatter mentioned above as opposed to general curvature in the plot of log E versus ρ. The modulus–density relation in Figure 2 is virtually indistinguishable from similar results obtained by Sperati et al.[2] for branched polyethylenes with $0.90 \leq \rho \leq 0.94$ g/cm^3 and by Krigas et al.[7] for HPB and linear polyethylene covering the range $0.86 \leq \rho \leq 0.95$ g/cm^3. Both absolute magnitudes and density dependence of E are similar to other studies where modulus was measured in uniaxial extension.[3-5,9] Dynamic mechanical results[8] give somewhat high E, presumably because of the higher frequency of the test.[3] Relatively few data are available for E in the density range above $\rho > 0.96$ g/cm^3, though such values fall below the extension of the line in Figure 2.[9] When converted to tensile modulus with a reasonable estimate of isotropic Poisson's ratio ($\nu = 0.33$), E from Illers' measurements on polyethylene of very high density are conspicuously below this extension. The significance of this deviation will be discussed below.

While the correlation of log E with density suggests some common determinant of the modulus for polyethylenes of different chemical microstructures, the question remains as to the nature or origin of this relation. The two-phase model can be used to relate density to crystallinity by the relation

$$\alpha = \frac{\rho - \rho_a}{\rho_c - \rho_a} \tag{3}$$

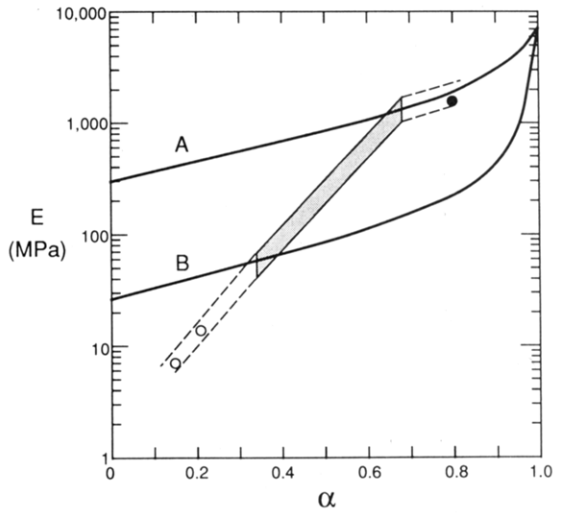

Figure 3. Semilogarithmic plot of modulus versus crystallinity. Present data are represented by hatched area, supplemented by points for lower[7] and higher[40] crystallinity. Lines are calculated with eq 4 with $E_c = 7$ MPa and $\xi = 1$: $E_a = 300$ MPa (A); $E_a = 27$ MPa (B).

This has been done with $\rho_c = 1.00$ g/cm^3 and ρ_a and 0.85 g/cm^3 to establish the upper abscissa in Figure 2. Neglecting the small change in ρ_c for HPB is not a serious oversight in the exercise to follow. It appears that the modulus of semicrystalline polyethylene conforms to eq 1, at least over the range of crystallinity studied here. Recall, however, that there is no theoretical basis for this semilogarithmic mixing rule. The apparent moduli for the amorphous and crystalline phases, obtained by extrapolating the data in Figure 2 to $\rho = 0.85$ g/cm^3 and $\rho = 1.00$ g/cm^3, are $E = 2$ MPa and $E = 28$ GPa, respectively. These are of the same orders of magnitude as the phase moduli $E_a = 6$ MPa and $E_c = 7$ GPa obtained from room temperature shear moduli in Table I and reasonable estimates of Poisson's ratio. It is believed that the correspondence of the data to eq 1 is fortuitous, resulting from the modulus of the amorphous phase changing with crystallinity. The semilogarithmic format is retained as a convenience for viewing large changes in E.

The lamellar averaging scheme of Boyd[19] is not employed here, as it has been demonstrated that similar behavior is obtained with the more convenient semiempirical Tsai-Halpin equation for two-phase mixtures.[23] For the case of the tensile modulus of semicrystalline polyethylene, this relation can be written as[39]

$$E = \frac{E_a[E_c + \xi(\alpha E_c + (1 - \alpha)E_a)]}{\alpha E_a + (1 - \alpha)E_c + \xi E_a} \tag{4}$$

Here E_c and E_a are composition-independent moduli of phases having volume fractions α and $(1 - \alpha)$, respectively, and ξ is an adjustable parameter. Reuss averaging is recovered for $\xi = 0$, and very large values of ξ lead to Voigt averaging. As discussed in the Introduction, G_c (and hence $E_c = 7$ GPa) is well established for polyethylene at room temperature. The experimental dependence of E on α cannot even be approximated by eq 4 for any values of the two remaining parameters E_a and ξ.

This is taken as strong evidence that E_a is not a constant; the stiffness of the amorphous component drops appreciably as crystallinity is lowered. Figure 3 summarizes a simple analysis of this effect. The hatched region represents the full extent of the present data. The upper curve "A" is the Tsai-Halpin equation with $E_c = 7$ GPa, $E_a = 300$ MPa, and $\xi = 1$. These values are not fitted to the present results but correspond to those used by Boyd to analyze

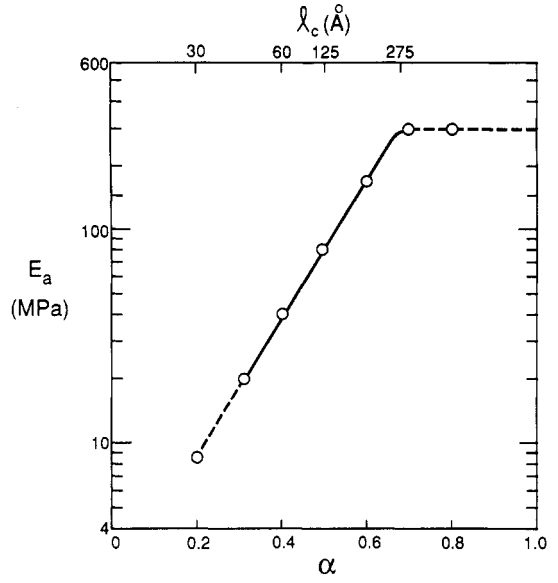

Figure 4. Dependence of E_a on crystallinity, as determined from eq 4 and data in Figure 4. Representative crystal thickness l_c is indicated.

Illers' data with both the Tsai-Halpin equation[23] and the lamellar composite averaging scheme.[19] Curve "A" thus represents Illers' data converted from shear to tensile moduli ($0.5 \leq \alpha \leq 0.96$). It is seen to account for the highest α portion of the present results, though a 3-fold discrepancy appears as α is decreased to 0.5. This difference is attributed to the higher frequency of the dynamic mechanical measurement, a point which is considered below. To fit the low crystallinity end of the data band in Figure 3, an appreciably smaller E_a is required. If $\xi = 1$ is retained to simulate constant stress lamellar averaging,[19] curve "B" represents the behavior for $E_a = 27$ MPa. The purpose of Figure 3 is to demonstrate graphically the case for a crystallinity dependent E_a contributing to the room temperature modulus of polyethylene. This conclusion is not dependent on the details of the composite model used to analyze the crystallinity dependence of E, though it is believed that eq 4 gives an accurate representation. The data range has been extended by including in Figure 3 points for two low crystallinity HPB samples from ref 7 and a more crystalline polyethylene.[40] These suggest that E_a continues to decrease for $\alpha < 0.3$. More interesting is the datum for $\alpha = 0.8$, which confirms that E_a is nearly constant at 300 MPa for $\alpha > 0.7$.

The crystallinity dependence of E_a, obtained by fitting eq 4 with $E_c = 7$ GPa and $\xi = 1$ to the hatched and outlined regions of Figure 3, is summarized in Figure 4. One notices that the shape of the log E_a–α curve mimics that of the total modulus in Figure 3. This is a natural consequence of the relatively high compliance of the amorphous phase. For $E_a \ll E_c$, eq 4 becomes

$$E = E_a(1 + \xi\alpha)/(1 - \alpha) \tag{5}$$

With $\xi = 1$, the α-dependent quotient varies by only a factor of 3 over the crystallinity range $0.3 \leq \alpha \leq 0.7$. It is clear that most of the 35-fold change in E over this range (see Figure 3) results from the decrease of E_a with decreasing crystallinity.

Hence it is demonstrated that the observed dependence of polyethylene's room temperature modulus on density (or crystallinity) is due largely to the strong increase of amorphous modulus E_a with α for crystallinity ≤ 0.7. In polyethylenes of higher crystallinity the amorphous modulus is effectively constant. The latter conclusion is based on composite response very near the constant stress "lower bound", an assumption which is justified by first principles calculations in the limit of complete crystallinity (see Table I). The former conclusion regarding the α-dependence of E_a is independent of any such assumption. The present analysis is done with $\xi = 1$ in eq 4 to be consistent with the established constant-stress behavior at high crystallinities.

The obvious question to be addressed is, why does E_a depend on α at small to moderate crystallinities but not at high crystallinity? To assist in answering this, representative crystal thickness l_c[35] has been indicated along the top of Figure 4. Amorphous layer thickness l_a, similarly calculated as the product of long period and noncrystalline fraction, is essentially constant at 105 ± 20 Å. There are two basic approaches for considering crystallinity effects on amorphous modulus E_a. The first involves perturbation of the normal or bulk rubbery behavior by the presence of lamellar crystals. The Krigbaum model[20,21] does in fact predict a strong positive dependence of E_a on α. But this scheme, as formulated, is based on a "fringed micelle" morphology which is generally considered inappropriate for semicrystalline flexible chain polymers. If modified to allow for chain folding, the model would predict a positive dependence of E_a on molecular weight corresponding to the increased number of "tie molecules". This, of course, is contrary to the observation that molecular weight has no effect on E, aside from a possible influence on crystallinity. Confinement of a rubbery polymer between platelike crystals can also decrease compliance be altering conformational statistics of the chains[41] or by coupling tensile modulus to the much larger bulk modulus. Regardless of the magnitude of such effects, stiffening of the amorphous component would be greatest for small amorphous layer thicknesses. The appreciable increase in E_a (see Figure 4) occurs in polyethylenes and copolymers having nearly constant l_a, so these mechanisms are not considered further.

The second approach for treating the strong dependence of E_a on α is related to viscoelasticity or, more precisely, mechanical relaxations occurring in polyethylene. These have been reviewed by Boyd.[42] Of prime interest here is the mechanical α_1 relaxation (not to be confused with the crystallinity α). This is ascribed to thermally activated motion of a defect such as a twist or kink along [001] in polyethylene crystals and coupling of resulting crystal stem mobility to the amorphous segments (loops and ties) in such a way as to relieve considerably the constraints on amorphous segments. In other words, the crystal defect motion activated in the mechanical α_1 process provides additional compliance mechanisms for amorphous segments. These result in a drop in E_a of at least an order of magnitude, as inferred from the temperature dependence of G_a reported in Boyd's analyses[19,23] of Illers' data. The other feature is that the temperature domain of the α_1 process, when measured at a fixed frequency, depends on crystal thickness l_c. It is well established that the thickness dependence of the α_1 temperature is pronounced for l_c less than 100 Å, becoming so small as to be barely perceptible for l_c greater than ca. 300 Å.[8,42-44] Schematic representations of the mechanical α_1 loss peak, based on measurements at 1 Hz,[8,42,45] are given for various crystal thicknesses in Figure 5.

With this background the behavior in Figure 4 becomes understandable, at least in a qualitative sense. The significant abscissa is that for crystal thickess l_c, not crystallinity α, though they are related by

$$\alpha = l_c/(l_c + l_a) \tag{6}$$

and l_a is nearly constant at ~105 Å for the homopolymers

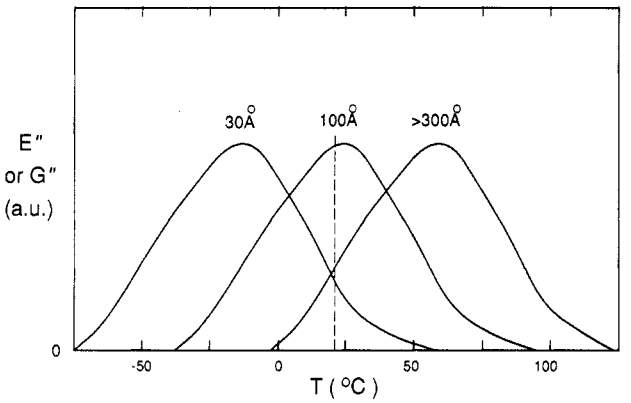

Figure 5. Schematic representation of the mechanical α_1 loss peak for polyethylenes of different l_c. Curve shape based on ref 45; temperature shifts from ref 8 and 42. Room temperature is indicated by vertical dashed line.

and copolymers studied here. For room temperature modulus measurements, the temperature location of the α_1 process determines the extent to which amorphous segments are relaxed, and hence E_a. Polyethylenes with l_c large enough to suppress the temperature shift of the mechanical α_1 relaxation (see the right-hand curve in Figure 5) have amorphous regions which are only slightly relaxed. E_a is large (~300 GPa) and independent of crystallinity, so the usual composite theories[19,23] predict correctly the observed dependence of modulus on crystallinity α. This situation changes when l_c becomes small enough to change the temperature location of the α_1 process, as indicated by the middle curve in Figure 5. At room temperature the α_1 relaxation is proportionally more activated (or the α_1 frequency is higher), leading to increased mobilization of the amorphous segments and a lowering of E_a. The left-most curve in Figure 5 indicates that the α_1 relaxation is nearly fully activated and that E_a should be near its relaxed or bulk room temperature value for l_c = 30 Å.

The scheme outlined above accounts in a self-consistent manner for the strong dependence of modulus on "crystallinity" for $\alpha < 0.7$ and the much weaker dependence at higher crystallinities, as summarized in Figure 4. It also explains systematic differences between dynamic mechanical results (~1 Hz) and moduli from uniaxial extension ($\dot{\epsilon} \approx 10^{-3}$ s^{-1}). Compare curve "A" of Figure 3, which represents the 1-Hz data of Illers[6] for linear polyethylene with $\alpha \geq 0.45$, to the data band for the present tensile results. With the higher frequency dynamic tests, a smaller l_c is required to start changing E_a at room temperature via the α_1 relaxation. Hence constant (unrelaxed) E_a behavior is retained to lower values of α or l_c, accounting for both a higher modulus and a more moderate "crystallinity" dependence. One supposes that the dynamic modulus would break below the behavior represented by curve "A" at a suitably small l_c, though that limit was not achieved in Illers' experiments with linear polyethylene, even at temperatures as high as 100 °C. Some branched polymers were studied in that same work;[6] their behavior is in qualitative accord with the present results, with the room temperature modulus falling appreciably below the constant E_a line for $\alpha < 0.7$. This is reasonable in light of the smaller l_c expected for short-chain branched copolymers. More quantitative comparison cannot be made to those data, since no information was supplied on molecular composition or morphology of the copolymers.

In this work we make no attempt to analyze in detail the relaxation of E_a by the mechanical α_1 process. It is noted that such relaxation occurs efficiently in short-chain

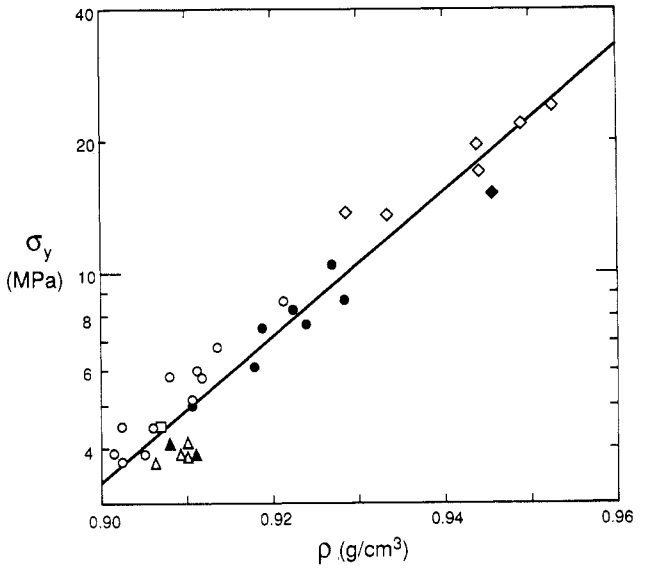

Figure 6. Relation of tensile yield stress to sample density. Line is linear least-squares fit to data. Symbols are for PE (◇), linear HPB (○), 3S HPB (△), and 4S HPB (□). Solid symbols are for polydisperse samples.

branched polymers, i.e., HPB's. Long-range translational diffusion of crystalline stems, which presumably is suppressed by branching, appears not to be required for achieving the observed lowering of E_a. It is possible that other dynamic mechanisms (e.g., the β process or the higher temperatures α' process) or structural features such as crystalline–amorphous interfaces influence the observed behavior. But it has been shown here that changes in the room temperature modulus are dominated by changes in E_a, and that the response of E_a to morphology and measuring frequency results from the mechanical α_1 process.

Yield Stress. The yield stress in Tables II and III are plotted in Figure 6 as a logarithmic function of density. This format was selected on purely empirical grounds; it is seen that yield stresses for both HPE and PE are well represented by one line. As with the modulus E there is some scatter (correlation coefficient is 0.97), but the yield stress seems to follow a single relation with density or crystallinity in this set of polyethylenes having various branching and molecular weights. While semilogrithmic formats are used for graphical presentations of modulus (Figure 2) and yield stress (Figure 6), no fundamental relation between the two should be inferred. Indeed the yield stress is less sensitive to density, changing by a factor of 6 over the range studied, as opposed to a factor of 20 for the modulus E. Extrapolating the present data, one obtains limiting values of 0.47 MPa and 158 MPa for σ_y at $\rho = 0.85$ g/cm^3 and $\rho = 1.00$ g/cm^3, respectively, though no particular significance is ascribed to these quantities.

What appears to be the crystallinity dependence of σ_y is treated here in terms of the minimum stress required to shear the polyethylene crystals by a dislocation mechanism and the relation of this stress to crystal thickness l_c. The noncrystalline component is not considered for the most part, its presence being required only to transmit forces by rubberlike elasticity. It will be shown that this approximation is quite reasonable for temperatures above that of the γ process (ca. 150 K), where the amorphous modulus is appreciably less than that of the crystals.

The model is that of yielding by $(hk0)[001]$ slip, resulting from homogeneously nucleated [001] screw dislocations under the combined effects of a shear stress τ and thermal energy. A brief account of this scheme has been presented

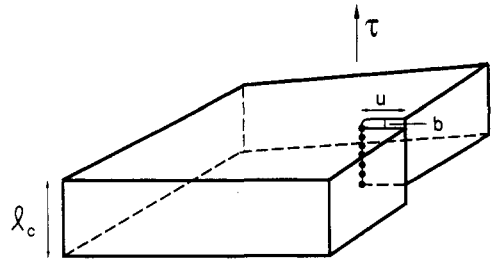

Figure 7. Sketch of [001] screw dislocation nucleus of dimension u. Dislocation length is equal to crystal thickness l_c. Magnitude of Burgers vector b is exaggerated.

earlier.[46] It has been shown by analytical calculations[29,47] and computer simulation[48] of dislocation energies that [001] screws are the most probable dislocations formed in polyethylene and that their line tension is too high to permit multiplication under stress fields. Hence nucleation must be relied upon to achieve crystal deformation by $(hk0)[001]$ slip.

A sketch of the geometry is shown in Figure 7 for a [001] screw dislocation which nucleated on a free $(hk0)$ surface and advanced a distance u into the crystal. The dislocation length is equal to the crystal thickness l_c. The Burgers vector is parallel to the dislocation and has magnitude b = 2.54 Å, the c-axis dimension of the polyethylene unit cell. Consideration is given here to the shear stress τ required to form a nucleus of critical size u^*. It is assumed that slip bands of size $u \geq u^*$ will continue to grow at a Peierls stress less than τ for nucleation. Constraints due to chain folding on the lamellar surfaces are ignored. Following Peterson,[49] we point out that the slip band need not be perfectly straight; the slip plane may change from one $(hk0)$ plane to another to avoid the impediment of a "tight" fold. This redirection could be achieved with little energy penalty, as the shear moduli for the various $(hk0)$ slip planes are similar.

The important quantity is the free energy associated with a nucleus such as that in Figure 7. Shadrake and and Guiu[29] write this as

$$\Delta G = \frac{\kappa b^2 l_c}{2\pi} \ln\left(\frac{u}{r_0}\right) - l_c b u \tau \qquad (7)$$

Here κ represents the elastic constants appropriate for $(hk0)[001]$ slip. Equation 7 applies also for a nucleus of two dislocations separated by a distance u in the central part of the crystal; nucleation and growth from a free $(hk0)$ surface are not required. The first term is the elastic strain energy (neglecting any contribution from the dislocation core of radius r_0), while the second is the irreversible work done by the applied shear stress τ. Some comments on the strain energy term are presented in the Appendix.

The analysis proceeds by setting equal to zero the derivative of ΔG with respect to u, establishing ΔG^*, the activation barrier for creating a nucleus of critical size u^*:

$$\Delta G^* = \frac{\kappa b^2 l_c}{2\pi}\left[\ln\left(\frac{u^*}{r_0}\right) - 1\right] \qquad (8)$$

where $u^* = \kappa b/2\pi\tau$. This activation energy, ΔG^*, which depends on stress through u^*, must be supplied by thermal fluctuations. Hence ΔG^* is proportional to kT, the thermal energy represented by the product of Boltzmann's constant and absolute temperature. Peterson[49] has shown that ΔG^* should be on the order of $40kT$ to achieve nucleation in laboratory time scales. It should be underscored that ΔG^* is not arbitrarily adjustable; it must correspond to probable

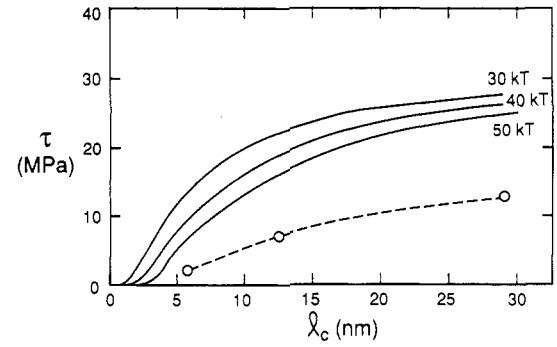

Figure 8. Resolved shear stress at yield, τ, versus l_c. Solid lines are calculated for indicated values of ΔG^*.

energies from thermal fluctuations, restricting it to $30kT \leq \Delta G^* \leq 50kT$. Decreasing ΔG^* by $10kT$ in this range is equivalent to increasing the strain rate by about 3 orders of magnitude. It will be shown that the exact choice of ΔG^* is not of prime importance. Having established ΔG^*, it is straightforward to evaluate u^* from eq 8 and hence the critical shear stress for nucleation:

$$\tau = \kappa b/2\pi u^* \qquad (9)$$

All quantities describing the model in eq 8 and 9 are known, except the exact value of ΔG^*. We impose transverse isotropy on the orthorhombic polyethylene crystal by letting $\kappa = (C_{44}C_{55})^{1/2}$. This is consistent with the spirit of eq 7, in which strain energy is based on isotropic elasticity. Hence we are considering an average over slip planes such as (100), (010), (110), etc., in the [001] slip direction. The temperature-dependent shear moduli of McCullough and Peterson[50] are used to compute κ, which ranges from 3.08 GPa (100 K) to 2.27 GPa (300 K). When compared at low temperatures, this κ is within 17% of the average calculated by others.[15,16] Given the agreement between experimental and calculated elastic moduli (Table I), κ is known in absolute terms to ±15%. The remaining quantity is the dislocation core radius r_0. Computer simulations of various [001] screw dislocations in polyethylene give $r_0 = 10 \pm 1$ Å.[47] One notes that this is equal to nearly twice the spacing between neighboring planes of chains and thus is consistent with the approximation $r_0 \approx 2b$ for isotropic crystals.

Representative values of σ_y from Table II are converted to maximum resolved shear stress, $\tau = \sigma_y/2$, and plotted versus crystal thickness l_c in Figure 8. These data are essentially the same as those found by Popli and Mandelkern.[9] This treatment of yielding implies a uniform stress field in semicrystalline polyethylene, a concept verified by the relation between elastic modulus and crystallinity (Reuss average) discussed in the preceding sections. Also shown in Figure 8 are calculated values of the theoretical strength τ from eq 8 and 9. The calculated values approximate the experimental magnitude and l_c dependence rather well, though theoretical strengths are about 2.5 times larger than observed. It should be emphasized that the calculation involves no adjustable parameters, aside from the variation of ΔG^* within reasonable bounds. No attempt has been made to "fit" theory to experiment by judicious selection of b, r_0, or κ. Furthermore, the calculated values of u^* are in the range 35–120 Å, which is less than the coherence length of $(hk0)$ planes in polyethylene. Results based on u^* greater than crystal dimensions would be unacceptable.

It could be argued that, given the simplicity of the model, agreement between experiment and theory is reasonable. But the origin of the discrepancy and a better

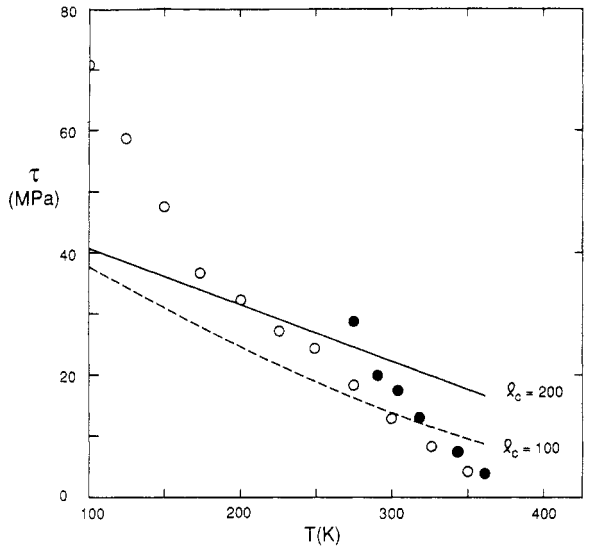

Figure 9. Temperature dependence of yield stress for polyethylene under uniaxial tension (○)[27] and plane strain compression (●).[28] Lines are calculated with $\Delta G^* = 50kT$ for indicated values of l_c.

appreciation of the role of dislocation nucleation and yielding in polyethylene are obtained from considering the temperature dependence of observed and calculated strengths. In Figure 9 the present theory is compared to the tensile yield results of Brown[27] for isotropic, linear polyethylene, $\rho = 0.964$ g/cm^3. Also shown are the results of Young[28] for specially textured linear polyethylene, $\rho = 0.966$ g/cm^3, $l_c \approx 200$ Å, deformed in plane strain compression by (010)[001] slip. Compression strength is a little larger than tensile yield strength. This may be due to different l_c, hydrostatic stress effects or the larger number of slip systems available in the isotropic tensile sample. The solid curve in Figure 9 is calculated for $\Delta G^* = 50kT$ and $l_c = 200$ Å, a reasonable figure for linear polyethylene with $\rho \approx 0.965$ g/cm^3 ($\alpha = 0.77$). The dashed curve for $l_c = 100$ Å indicates the sensitivity of τ to crystal thickness. About 35% of the drop in calculated strength between 100 and 360 K comes directly from the temperature dependence of the shear moduli.

Theoretical and experimental results are in good agreement over the limited temperature range 175–260 K. Here both the absolute magnitude of yield stress and temperature dependence are adequately reproduced by the dislocation nucleation model. It is emphasized once again that no attempt has been made to parameterize the model to fit the data. At both lower and higher temperatures the experimental yield stress is seen to vary more rapidly with temperature. These effects can be understood in terms of thermally activated motion of chain segments, or relaxation processes, in semicrystalline polyethylene.

As stated in the description of the model, macroscopic yielding is assumed to be controlled by the onset of slip within the lamellar crystals. This is reasonable provided the amorphous regions are compliant and weak compared to the crystals. As temperature is dropped toward 150 K, approaching the location of the γ process at 1 Hz, this is no longer the case; the modulus of the amorphous regions abruptly increases toward that of the crystals.[19,23] Yielding at such low temperatures thus depends on the ability to shear the amorphous regions as well. Brown[27] has suggested that this requires a higher stress than for intracrystalline slip because of the lack of dislocation mechanisms in rigid or "glassy" amorphous polyethylene. The clear departure of experiment from theory at $T \approx 150$ K certainly supports this idea. More germane to the present argument is that experimental and theoretical yield stress coincide at temperatures where they should, i.e., for $T >$ 150 K, where deformation and yield of amorphous regions can be neglected.

The discrepancies at $T > 260$ K are attributed to the onset of the α_1 process described in the section on elastic modulus. For crystals with $l_c = 200$ Å, the mechanical α_1 process commences very near 270 K at 1 Hz for thick crystals, the exact location depending on frequency or time scale of the measurement (see Figure 5). Here we concentrate on the axial chain mobility produced by the motion of twist or kink defects in the crystal. It must be appreciated that the abrupt onset of such mobility will enhance chain slip in the [001] direction. A very simple treatment of this effect is to decrease the size of the Burgers vector to $b = 1.27$ Å, corresponding to the reestablishment of crystallographic register after chain translation of $c/2$ when a twist or kink is present.[42,43] Applying this idea at $T = 360$ K where the α_1 process is most fully activated, calculated yield stress is reduced by a factor of 8 to $\tau = 2$ MPa, in reasonable accord with experiment.

More work clearly needs to be done on this high temperature region, where it appears that thermally activated generation of one type of defect (a dynamic twist or kink) modifies the energetics of a larger line defect (the [001] screw dislocation). We note that the l_c dependence of τ predicted by the dislocation model is shown by experiments at room temperature (Figure 6), where the α_1 process is at least partially activated. This suggests that a modified dislocation mechanism controls the yield stress at elevated temperature.

In closing this section it should be acknowledged that many possible complications have been overlooked. Other deformation mechanisms such as twinning and crystal–crystal phase transformations[51] have not been considered. Neither has the effect of short-chain branching, though the experimental data in Figure 9 and most of that in Figure 8 are for linear polyethylene. It is shown, however, that a simple dislocation model accounts quantitatively for observed shear strength in the temperature interval between 175 and 260 K (−98 to −13 °C), which is precisely where the model is expected to be most satisfactory. At lower temperature there is a "toughening" occasioned by vitrification of amorphous polyethylene segments, and at higher temperatures intracrystalline shear is facilitated by thermally generated twist or kink defects.

Conclusions

The oft-observed dependence of room temperature elastic modulus and yield stress on polyethylene's thermal history, comonomer content, etc. has been shown to result from changes in crystal thickness, l_c, as opposed to crystallinity. Most of the 20-fold variation in tensile modulus E displayed by polyethylenes with crystallinities within the conventional range $0.4 \leq \alpha \leq 0.7$ is attributed to the strong dependence of amorphous modulus E_a on crystal thickness by way of the mechanical α_1 relaxation process. If the amorphous modulus E_a were constant, stiffness of polyethylene would vary by a factor of only ~2 over the same crystallinity range. This constant E_a situation in fact obtains for $\alpha \geq 0.7$, where crystal thickness l_c is large enough to fix the extent of amorphous relaxation by the α_1 process.

Yielding of semicrystalline polyethylene is analyzed successfully in terms of nucleation of [001] screw dislocations in lamellar crystals. The model is quantitative with no disposable parameters. It accounts for observed yield stress in the temperature interval between the γ and α_1

relaxations; it represents the first absolute calculation of strength for a semicrystalline polymer. Above 260 K (including room temperature), experimental yield stress is significantly less than that calculated with the simple dislocation model. A plausible case is made for τ (or σ_y) being lowered by the α_1 process, and a reasonable estimate of this decrease is presented.

In summary, the prime determinant of small strain mechanical properties of polyethylene at room temperature is crystal thickness, l_c, which is related indirectly to crystallinity by the apparent constancy of amorphous layer thickness l_a. The dependence of modulus E on l_c results from the crystal thickness dependence of the mechanical α_1 process. Yield stress τ depends on l_c through the energetics for dislocation formation, which are modified at room temperature by partial activation of the α_1 process.

Acknowledgment. This research was supported by the Gas Research Institute, Physical Sciences Department (Contract 5084-260-1051), and by Northwestern's Materials Research Center with funds provided by NSF's MRL Program (DMR-85 20280). We thank C. Metaxas for supplying tensile data on some of the linear polyethylenes and Prof. W. W. Graessley for assistance in obtaining hydrogenated polybutadiene samples.

Appendix

The elastic strain energy of the dislocation nucleus in eq 7 is

$$E(l_c) = \frac{Kb^2}{2\pi} \ln\left(\frac{u}{r_0}\right) \qquad \text{(A-1)}$$

Here the thickness dependence comes solely from the length of the dislocation, l_c. Equation A-1 is correct in the limit $u \ll l_c$. A more complete treatment includes consideration of the fact that the basal (001) surfaces of the lamellar crystal are under no net force. The energetics of a [001] screw dislocation running parallel to the surface normal in a thin crystal was addressed by Eshelby and Stroh,[52] and certain of their results were used by Peterson[49] and Young.[28] In general terms, the requirement that stress and local energy density vanish at the free surface reduces $E(l_c)$ below that in eq A-1.

Peterson[49] wrote an expression for $E'(l_c)$ (which will not be reproduced here) which was intended to account for finite thickness effects on the strain field in the lamellar crystal. One mathematical approximation used by Peterson is valid only for $u < 0.16l_c$, where surface effects are moderate and eq A-1 is a reasonable approximation. More importantly, Peterson's $E'(l_c)$ is for an isolated dislocation, not a nucleus of two dislocations or one dislocation interacting with a free $(hk0)$ surface. The magnitude of the strain energy is thus reduced by at least 50%, making dislocations unrealistically easy to form. This is the major reason for difficulties encountered by Peterson[49] and Young[28] using nucleation theory with the underestimate $E'(l_c)$.

Returning to the present analysis, it should be pointed out that the simple expression for $E(l_c)$ is an approximation which is rigorously correct only when $u \ll l_c$. The calculated values of τ in Figure 9 correspond to $u^* < 35$ Å in the important range $T > 150$ K. For $l_c = 200$ Å, $u^* < 0.17l_c$ and eqn 7–9 are expected to be reasonably correct. For $l_c \leq 100$ Å the strain energy and hence calculated values of τ in Figures 8 and 9 are probably too large by a significant factor (ca. 100%). A more complete analysis of surface effects, based on the formulation of Eshelby and Stroh,[52] is required for the case of very thin polyethylene crystals. Such an analysis is beyond the scope of this work. It is emphasized, however, that the conclusions drawn here, particularly those regarding the yielding of crystals with $l_c \approx 200$ Å, are essentially correct.

Registry No. PE, 9002-88-4.

References and Notes

(1) Crist, B.; Fisher, C. J.; Metaxas, C. Manuscript in preparation.
(2) Sperati, C. A.; Franta, W. A.; Starkweather, H. W. *J. Am. Chem. Soc.* **1953**, *75*, 6127.
(3) Sandiford, D. J. H.; Willbourn, A. H. In *Polythene*, 2nd ed.; Renfrew, A., Morgan, P., Eds.; Interscience: New York, 1960; pp 167–229.
(4) Tung, L. *SPE J. 1958*, July, 25–28.
(5) Boenig, H. V. *Polyolefins*; Elsevier: New York, 1966; Chapter 4.
(6) Illers, K. H. *Kolloid Z. Z. Polym.* **1973**, *251*, 394.
(7) Krigas, T.; Carella, J. M.; Struglinski, M. J.; Crist, B.; Graessley, W. W.; Schilling, F. C. *J. Polym. Sci., Polym. Phys. Ed.* **1985**, *23*, 509.
(8) Khanna, Y. P.; Turi, E. A.; Taylor, T. J.; Vickroy, V. V.; Abbott, R. F. *Macromolecules* **1985**, *18*, 1302.
(9) Popli, R.; Mandelkern, L. *J. Polym. Sci., Polym. Phys. Ed.* **1987**, *25*, 441.
(10) Williamson, G. R.; Wright, B.; Haward, R. N. *J. Appl. Chem.* **1964**, *14*, 131.
(11) Bowden, P. B.; Young, R. J. *J. Mater. Sci.* **1974**, *9*, 2034.
(12) Trainor, A.; Haward, R. N.; Hay, J. N. *J. Polym. Sci., Polym. Phys. Ed.* **1977**, *15*, 1077.
(13) Davis, G. T.; Eby, R. K. *J. Appl. Phys.* **1973**, *44*, 4274.
(14) Odajima, A.; Maeda, T. *J. Polym. Sci.* **1966**, *C15*, 54.
(15) Wobser, G.; Blasenbrey, S. *Kolloid Z. Z. Polym.* **1970**, *241*, 985.
(16) Sorenson, R. A.; Liau, W. B.; Kesner, L.; Boyd, R. H. *Macromolecules* **1988**, *21*, 200.
(17) Hellwege, K. H.; Knappe, W.; Lehman, P. *Kolloid Z. Z. Polym.* **1962**, *183*, 110.
(18) Graessley, W. W. *Adv. Polym. Sci.* **1982**, *47*, 67.
(19) Boyd, R. H. *J. Polym. Sci., Polym. Phys. Ed.* **1983**, *21*, 493.
(20) Krigbaum, W. R.; Roe, R. J.; Smith, K. J. *Polymer* **1964**, *5*, 533.
(21) Krigbaum, W. R. *J. Polym. Sci.* **1966**, *C15*, 251.
(22) Gray, R. W.; McCrum, G. N. *J. Polym. Sci., Part A-2* **1969**, *7*, 1329.
(23) Boyd, R. H. *Polym. Eng. Sci.* **1979**, *19*, 1010.
(24) Phillips, P. J.; Patel, J. *Polym. Eng. Sci.* **1978**, *18*, 943.
(25) Matsuoka, S. In *Failure of Plastics*; Brostow, W., Corneliussen, R. D., Eds.; Hanser Publishers: New York, 1986; Chapter 3.
(26) Young, R. J.; Bowden, P. B.; Ritchie, J. M.; Rider, J. G. *J. Mater. Sci.* **1973**, *8*, 23.
(27) Brown, N. In *Failure of Plastics*; Brostow, W., Corneliussen, R. D., Eds.; Hanser Publishers: New York, 1986; Chapter 6.
(28) Young, R. J. *Philos. Magn.* **1974**, *30*, 85.
(29) Shadrake, L. G.; Guiu, F. *Philos. Magn.* **1976**, *34*, 565.
(30) Juska, T.; Harrison, I. R. *Polym. Eng. Rev.* **1982**, *2*, 13.
(31) Rachapudy, H.; Smith, G.; Raju, V. R.; Graessley, W. W. *J. Polym. Sci., Polym. Phys. Ed.* **1979**, *17*, 1211.
(32) Raju, V. R.; Rachapudy, H.; Graessley, W. W. *J. Polym. Sci., Polym. Phys. Ed.* **1979**, *17*, 1223.
(33) Tanzer, J. D.; Bartels, C. R.; Crist, B.; Graessley, W. W. *Macromolecules* **1984**, *17*, 2708.
(34) Richardson, M. J.; Flory, P. J.; Jackson, J. B. *Polymer* **1963**, *4*, 221.
(35) Howard, P. R. Ph.D. Thesis, Northwestern University, 1987.
(36) Mandelkern, L.; Glotin, M.; Benson, R. A. *Macromolecules* **1981**, *14*, 22.
(37) Crist, B.; Wignall, G. D. *J. Appl. Cryst.*, in press.
(38) Tanzer, J. D.; Crist, B.; Graessley, W. W. *J. Polym. Sci., Polym. Phys. Ed.*, in press.
(39) McCullough, R. L. In *Treatise on Materials Science and Technology*; Schultz, J. M., Ed.; Academic Press: New York, 1977; Vol. 10, pp 453–540.
(40) Metaxas, C. Private communication.
(41) Lohse, D. J.; Gaylord, R. J. *Polym. Eng. Sci.* **1978**, *18*, 513.
(42) Boyd, R. H. *Polymer* **1985**, *26*, 323, 1123.
(43) Mansfield, M.; Boyd, R. H. *J. Polym. Sci., Polym. Phys. Ed.* **1978**, *14*, 1227.
(44) Popli, R.; Glotin, M.; Mandelkern, L.; Benson, R. S. *J. Polym. Sci., Polym. Phys. Ed.* **1984**, *22*, 407.
(45) Pechhold, W.; Eisele, U.; Knauss, G. *Kolloid Z. Z. Polym.* **1964**, *196*, 27.
(46) Crist, B. *Polym. Commun.*, in press.
(47) Shadrake, L. G.; Guiu, F. *Philos. Magn. A* **1979**, *39*, 785.
(48) Bacon, D. J.; Tharmalingam, K. J. *J. Mater. Sci.* **1983**, *18*, 884.

(49) Peterson, J. M. J. Appl. Phys. 1966, 37, 4047.
(50) McCullough, R. L.; Peterson, J. M. J. Appl. Phys. 1973, 44, 1224.
(51) Young, R. J. In Developments in Polymer Fracture; Andrews, E. H., Ed.; Applied Science Publishers: London, 1979; Vol. 1, Chapter 7.
(52) Eshelby, J. D.; Stroh, A. N. Philos. Magn. 1951, 42, 1401.
(53) Note added in proof: A similar analysis of polyethylene yielding at room temperature by dislocations has been presented recently: Young, R. J. Materials Forum, in press.

The Photoluminescence of Poly(methylphenylsilylene). The Origin of the Long-Wavelength Broad Band

O. Ito, M. Terazima, and T. Azumi*

Department of Chemistry, Faculty of Science, Tohoku University, Sendai 980, Japan

N. Matsumoto, K. Takeda, and M. Fujino

Electrical Communications Laboratories, NTT, Musashino, Tokyo 180, Japan.
Received April 13, 1988; Revised Manuscript Received September 1, 1988

ABSTRACT: The photoluminescence of poly(methylphenylsilylene) consists of a relatively sharp band at 350 nm and a significantly broad band in the 400–500-nm region. The luminescence behavior is investigated at low temperatures in an effort to identify the origin of the long-wavelength broad emission. The excitation spectra differ for the sharp and the broad emission bands: The broad emission band is more enhanced when the excitation is carried out at the π,π^* absorption band of the phenyl substituent as compared to the excitation at the σ,σ^* absorption band of the silicon skeleton. The lifetimes are of the order of picoseconds for both the sharp and the broad bands. The intensity of the broad emission monotonically decreases as the temperature increases from 4.2 K to ~180 K, whereas the intensity of the sharp emission remains nearly constant. From these experiments together with the previous theoretical considerations we conclude that the broad emission band is an emission from the intrapolymer skeleton σ to pendant π^* charge transfer state.

1. Introduction

The photoluminescence of poly(methylphenylsilylene), $(CH_3C_6H_5Si)_n$ (often referred to as methylphenylpolysilane), was first reported by Kagawa et al.[1] The luminescence is composed of two bands: a relatively sharp (fwhm ~500 cm^{-1}) band at 350 nm and a significantly broad (fwhm ~5000 cm^{-1}) and structureless band in the 400–500-nm region. The sharp band in the short-wavelength side is also observed for poly(methylpropylsilylene) and is understood to be the σ^*,σ interband transition delocalized over the silicon skeleton. The broad band in the long-wavelength side, on the other hand, is observed only when phenyl groups are substituted on the silicon skeleton.

Two different mechanisms for this broad luminescence have been proposed. Kagawa et al.[1] ascribed it to an emission from a charge-transfer state between the silicon skeleton and the phenyl pendants. Harrah and Zeigler,[2] on the other hand, claimed that the broad luminescence was due to an impurity generated by photolysis of the polymer.

In the present paper, we try to make a more conclusive assignment of the broad luminescence located in the long-wavelength region. To this end, various spectroscopic measurements were carried out at very low temperatures, under which condition any photodegradation of the polymer is unlikely to take place. As will be discussed in detail below, we conclude that the broad luminescence is due to a charge-transfer state between the skeleton σ orbital delocalized over the whole silicon chain and the pendant π^* orbital.

For the sake of brevity, the two types of emission bands will hereafter be referred to simply as "the sharp band" and "the broad band".

2. Experimental Section

Poly(methylphenylsilylene) was prepared by polymerization of methylphenyldichlorosilane using sodium metal in boiling toluene in a manner described by West.[3] The crude polymer thus prepared was purified first by washing with methanol and then by the freeze dry method. The molecular weight distribution measured by gel permeation chromatography is shown in Figure 1. The maximum is found at a molecular weight of 1.2×10^5. The synthesized polymer was further fractionated into different molecular weights by a Shodex GPC-A-804 gel permeation chromatograph. All the processes of synthesis, purification, and measurements were carried out under yellow light so that any photochemical degradation of the polymer is inhibited.

The emission was investigated for both *p*-dioxane solutions (concentration of 1.6×10^{-3} M with respect to Si atom) and films. Dioxane used as a solvent was purified by fractional distillation. The films were prepared by the spin coating on a SiO_2 substrate. The molecular weight of the polymer used in the film was 0.7×10^5.

The emission spectra were obtained with a $^3/_4$-m Spex 1702 monochromator equipped with a Hamamatsu R928 photomultiplier tube. The excitation was carried out by light from a 500-W Xe lamp passed through a 30-cm Nalumi double monochromator. The excitation spectra were corrected for the wavelength dependence of the monochromator and the light distribution of the Xe lamp by means of a Rhodamine 6G quantum counter.

In the case of the decay measurements, the excitation was carried out by a Molectron UV-400 nitrogen laser. The decay signal was digitized by an Iwatsu DM-900 digital memory, and the digital data were transferred to a microcomputer for signal averaging.

The spectra were measured at various temperatures between 4.2 and ~180 K. The temperatures above the liquid helium temperature were controlled by an Osaka Sanso Cryomini-O closed cycle cryogenic system.

3. Results

(a) Emission and Excitation Spectra. Figure 2 shows the emission spectra observed for a dioxane solution and for a spin coated film at 4.2 K. The spectra are qualitatively similar to the spectrum observed by Kagawa et al.[1] for a coated film at 77 K. That is, the spectrum is composed of the sharp band in the short-wavelength side and the broad band in the long-wavelength side.

0024-9297/89/2222-1718$01.50/0